

# DYNAMICS OF FERRITE CAVITIES AND THEIR EFFECT ON LONGITUDINAL DIPOLE OSCILLATIONS\*

C. Spies<sup>†</sup>, U. Hartel, M. Glesner, TU Darmstadt, Darmstadt, Germany  
H.-G. König, H. Klingbeil, GSI, Darmstadt, Germany

## Abstract

In this paper, we consider ferrite cavities of the type that is currently used in the SIS18 at GSI and will be used in the future SIS100 which is being built in the frame of the FAIR project. We analyze the dynamics of the cavities in conjunction with their local control loops. An emphasis is put on the cavities' reaction to changes in the desired amplitude or resonant frequency. Using simulations, we show that the cavities' dynamics hardly influence longitudinal dipole oscillations, and conclude that a low-order model for the RF cavities is sufficient.

## FERRITE CAVITIES

In a heavy-ion synchrotron, the frequency of the RF accelerating fields is typically relatively low ( $< 10$  MHz) and highly variable [1]; for instance, in the planned SIS100 synchrotron at the GSI Helmholtz Centre for Heavy-Ion Research,  $^{238}\text{U}^{28+}$  ions will be injected at about  $0.56 \cdot c_0$  and accelerated to about  $0.92 \cdot c_0$ . Ferrite cavities for low RF frequencies are significantly smaller than, e. g. a  $\frac{\lambda}{2}$  resonator cavity, and their resonance frequency can be tuned.

In a ferrite cavity, the metal beam pipe is interrupted by a short ceramic "gap" and surrounded by ferrite rings. Bias and excitation loops are wound around the ferrite rings (see Fig. 1). The RF current excites an RF magnetic field in the ferrite rings, which in turn induces an RF electric field along the beam pipe. This field enters the ceramic gap and accelerates the charged particles. The RF field also effects a reactive current in the metal beam pipe and casing.

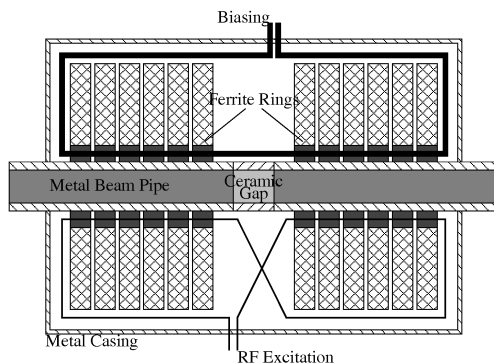


Figure 1: Schematic diagram of a ferrite cavity.

The cavity's behavior is equivalent to an RLC parallel oscillator (see Fig. 2) whose input is the RF excitation current [1]. The voltage across the RLC circuit is the voltage

\* Work supported by the German Ministry of Education and Research, Grant No. 06DA9028I

<sup>†</sup> christopher.spies@mes.tu-darmstadt.de

across the ceramic gap. The capacitance is primarily that of the ceramic gap and is constant. The inductance depends on the differential magnetic permeability of the ferrite material and can be tuned by the bias current. The resistance represents both Ohmic and magnetic losses and may be frequency and/or voltage dependent.

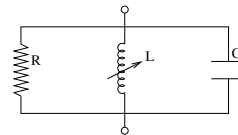


Figure 2: Equivalent circuit.

## Resonance Frequency Control

From the equivalent circuit in Fig. 2, it is obvious that the accelerating voltage is maximized when the cavity is operated at its resonant frequency. In that case, the voltage is in phase with the excitation current. Therefore, each cavity is equipped with a local controller that measures the phase difference between excitation current and gap voltage. It outputs a low-level voltage that controls a solid-state amplifier which in turn generates the bias current.

The controller is an analog circuit based on operational amplifiers (OpAmps) and has a linear *PI* characteristic, i. e. its step response is the sum of that of a proportional (*P*) and that of an integral (*I*) controller. Additionally, there is a pilot control path that nonlinearly maps the setpoint frequency to an approximation of the required bias current.

## Amplitude Control

Each cavity is also equipped with a local amplitude controller that measures the gap voltage (using a voltage divider) and compares it to the voltage setpoint. It outputs a low-level voltage that is used to modulate a low-level RF input signal, which is in turn fed into an amplifier chain that generates the excitation current.

The controller is an analog OpAmp circuit and has a linear *PPT*<sub>1</sub> characteristic, i. e. its step response is the sum of that of a *P* element and that of another *P* element with first-order lag (*PT*<sub>1</sub>). Additionally, there is a constant-gain pilot control path.

## Cavity Synchronization

Since the resonance frequency control described in section cannot detect phase shifts in the modulator-amplifier chain, another local controller measures the phase difference between the gap voltage and a reference signal and

adjusts the phase of the input signal in order to match the gap voltage's phase to that of the reference signal.

### NONLINEARITIES

Many of the involved components exhibit nonlinear characteristics, some of which have been summarized in tbls. 1, 2 and 3.

Table 1: Frequency Dependency of Modulator / Amplifier Characteristics

Frequency	Amplifier Gain	Phase Shift
0.8 MHz	55 S	8.6°
2.0 MHz	31 S	54°
4.0 MHz	33 S	115°

Table 2: Frequency Dependency of Resonance Frequency Control Characteristics

Frequency	Amplifier Gain	Pilot Control Error
1.0 MHz	128 S	-5%
2.0 MHz	200 S	-22%
3.0 MHz	380 S	-23%
4.0 MHz	420 S	-20%

Table 3: Frequency Dependency of a Cavity's Resonance Frequency

Frequency	Bias Current	Inductance
1.0 MHz	20 A	33.4 μH
2.3 MHz	100 A	6.3 μH
2.9 MHz	150 A	4.0 μH
3.9 MHz	250 A	2.3 μH
4.8 MHz	400 A	1.5 μH

Experiments have shown the resistance in Fig. 2 to depend both on the operating frequency and on the voltage across the cavity. Figure 4 visualizes this dependency.

### SYSTEM BEHAVIOR

Experiments conducted at GSI have shown that the amplitude control's plant (consisting of the amplitude modulator, the amplifier chain, the cavity and the voltage divider) exhibits a second-order frequency-dependent time lag of the order of some 10 ns and a dead-time of 3.9 μs. Only a part of the latter (about 1 μs) is caused by the cable delay to and from the cavity. The remainder must be attributed to an inherent dynamism of the plant.

The closed-loop resonance frequency control is capable of overshooting; its attenuation factor is 0.458, and its resonant frequency is 3.15 kHz in small-signal analyses.

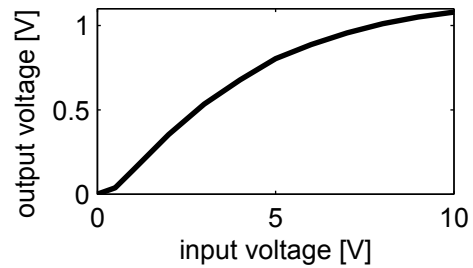


Figure 3: Modulator input-output characteristic.

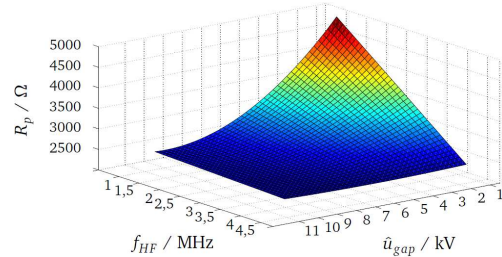


Figure 4: Cavity resistance.

Larger time constants are observed for larger steps in the frequency setpoint due to the limited slew rate of the bias current.

### SIMULATION MODELS

We created two different simulation models. Each includes 14 cavities as well as their local control loops. The cavities were assigned random parameter deviations of up to 20%. In the first model, all the known nonlinearities as well as the dynamism of the cavity with respect to the amplitude have been included; Spline interpolations between the data points in sec. were used. In the second model, all input-output characteristics have been assumed to be linear, and all gains have been assumed to be constant. Their values have been chosen such that the open-loop gain becomes identical to the minimum open-loop gain of the nonlinear system. Therefore, the closed-loop time constant of the linear model equals the worst-case time constant of the nonlinear model.

We used preliminary ramp data for the future SIS100 synchrotron (under construction at GSI) as an input to the simulation. Figure 5 shows the RF amplitude and RF frequency setpoints during a <sup>238</sup>U<sup>28+</sup> simulation cycle. We are primarily interested in the amplitude and phase of the effective RF voltage acting on the particles.

### SIMULATION RESULTS

Figure 6 shows the actual RF amplitude obtained by simulating the first model along with the difference between both simulations. The maximum difference is about 1.5 kV. The relative difference is below 1% of the total RF amplitude except at the very end of the simulation, after flat-top has been reached.

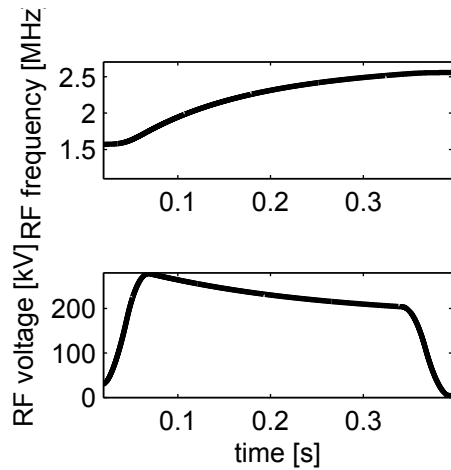


Figure 5: Frequency (top) and amplitude (bottom) ramps.

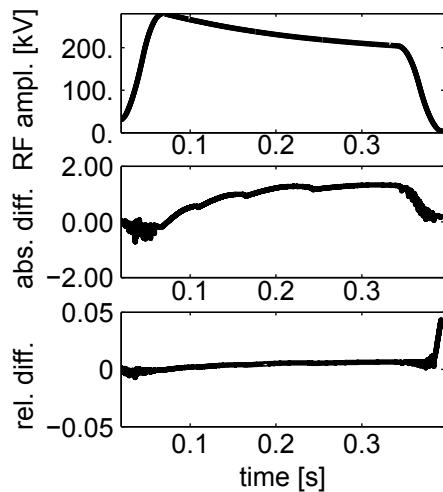


Figure 6: Actual RF amplitude (top), absolute difference (center) and relative difference (bottom).

Figure 7 shows the deviation of the RF phase from its setpoint in both simulations. The maximum deviation in both simulations is only about  $0.5^\circ$ , which is below the accuracy of about  $2^\circ$  that the cavity synchronization can achieve in practice [2]. This difference is hardly noticeable.

These results suggest that the aforementioned nonlinearities have little impact on the RF amplitude and phase and consequently should have little to no impact on the beam. We therefore also simulated the influence of the RF voltage on the longitudinal motion of a single macro-particle. The resulting deviation of the beam phase from its setpoint in both simulations is shown in Fig. 8. There is no quantitative difference between both plots.

## CONCLUSIONS

From the simulation results presented in this paper, we conclude that the second model (neglecting the nonlinearities) is a good fit. The local control loops mask the effect of the nonlinearities; the linear model would be a poor fit

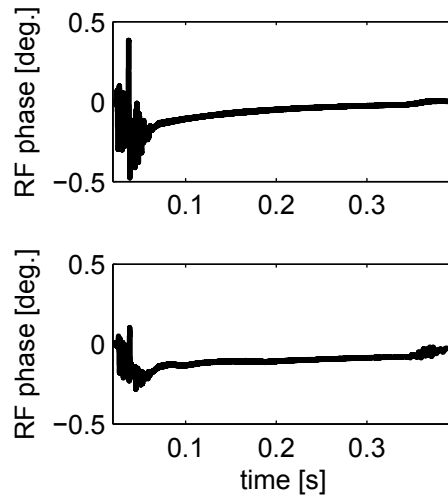


Figure 7: Actual RF phase.

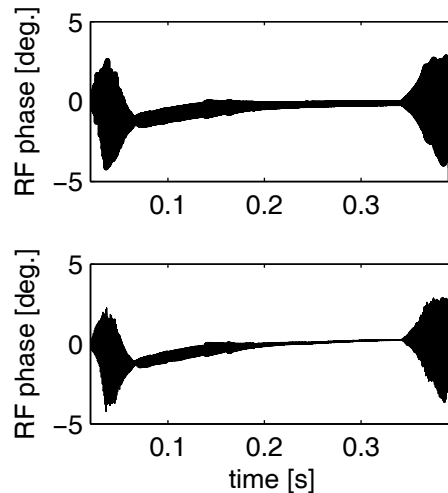


Figure 8: Beam phase.

for the open-loop system. Neglecting the nonlinearities reduced the required simulation time by about 20%.

## ACKNOWLEDGMENTS

The authors would like to thank Martin Kumm for the system identification of the amplitude control plant and Jörg Mohr and Thomas Wöber for determining the input-output characteristics of the amplitude modulator.

## REFERENCES

- [1] H. Klingbeil, "Ferrite Cavities," *Proc. CERN Accelerator School*, 2010, pp. 299–317.
- [2] H. Klingbeil, H. Damerau, M. Kumm, P. Moritz, G. Schreiber, B. Zipfel, "Commissioning of the SIS12/18 Cavity Synchronization System," GSI Scientific Report, 2005, p. 132.